Cell

Arc/Arg3.1 Regulates an Endosomal Pathway Essential for Activity-Dependent β-Amyloid Generation

Jing Wu,[1] Ronald S. Petralia,[5] Hideaki Kurushima,[1] Hiral Patel,[6] Mi-young Jung,[6] Lenora Volk,[1,4] Shoaib Chowdhury,[1] Jason D. Shepherd,[1,9] Marlin Dehoff,[1] Yueming Li,[7] Dietmar Kuhl,[8] Richard L. Huganir,[1,4] Donald L. Price,[1,2,3] Robert Scannevin,[6] Juan C. Troncoso,[2,3] Philip C. Wong,[1,3] and Paul F. Worley[1,2,*]

[1]Solomon H. Snyder Department of Neuroscience
[2]Department of Neurology
[3]Department of Pathology
[4]Howard Hughes Medical Institute
Johns Hopkins University School of Medicine, Baltimore, MD 21205, USA
[5]Laboratory of Neurochemistry, National Institute on Deafness and Other Communication Disorders, National Institutes of Health, Bethesda, MD 20892, USA
[6]Biogen Idec, 14 Cambridge Center, Cambridge, MA 02142, USA
[7]Molecular Pharmacology and Chemistry Program, Memorial Sloan-Kettering Cancer Center, New York, NY 10021, USA
[8]Institute for Molecular and Cellular Cognition, Center for Molecular Neurobiology (ZMNH), University Medical Center Hamburg-Eppendorf (UKE), Hamburg 20251, Germany
[9]Present address: The Picower Institute for Learning and Memory, Massachusetts Institute of Technology, Cambridge, MA, USA
*Correspondence: pworley@jhmi.edu
DOI 10.1016/j.cell.2011.09.036

SUMMARY

Assemblies of β-amyloid (Aβ) peptides are pathological mediators of Alzheimer's Disease (AD) and are produced by the sequential cleavages of amyloid precursor protein (APP) by β-secretase (BACE1) and γ-secretase. The generation of Aβ is coupled to neuronal activity, but the molecular basis is unknown. Here, we report that the immediate early gene *Arc* is required for activity-dependent generation of Aβ. Arc is a postsynaptic protein that recruits endophilin2/3 and dynamin to early/recycling endosomes that traffic AMPA receptors to reduce synaptic strength in both Hebbian and non-Hebbian forms of plasticity. The Arc-endosome also traffics APP and BACE1, and Arc physically associates with presenilin1 (PS1) to regulate γ-secretase trafficking and confer activity dependence. Genetic deletion of Arc reduces Aβ load in a transgenic mouse model of AD. In concert with the finding that patients with AD can express anomalously high levels of Arc, we hypothesize that Arc participates in the pathogenesis of AD.

INTRODUCTION

Alzheimer's Disease (AD) is the most common cause of dementia in the elderly and is characterized by a progressive loss of cognitive functions. The histopathology of AD includes accumulations of extracellular Aβ peptides (neuritic plaques) and intraneuronal hyperphosphorylated tau (neurofibrillary tangles) (Hardy and Selkoe, 2002). Several lines of evidence suggest that cognitive failure is linked to the generation and deposition of neurotoxic species of Aβ derived by secretase cleavage of the amyloid precursor protein (APP). APP is an integral type I membrane protein that is trafficked through a constitutive secretary pathway and processed at the cell surface, trans-Golgi network (TGN) and endocytic organelles (Thinakaran and Koo, 2008). β APP cleavage enzyme1 (BACE1) and the γ-secretase complex, which includes presenilin1 (PS1), Nicastrin, Aph-1, and Pen2, are also present in ER, TGN, endosomes, and on the cell surface (De Strooper and Annaert, 2010; Small and Gandy, 2006). Amyloidogenic processing of APP is thought to occur in endosomes, but the precise trafficking events remain unclear.

Aβ generation can be modulated by neural activity in the interstitial fluid (ISF) in vivo (Cirrito et al., 2005) or in hippocampal slices (Kamenetz et al., 2003), suggesting that a substantial fraction of Aβ generation is dependent on activity; however, the contribution of activity-dependent Aβ generation to amyloid deposition in vivo is as yet unclear. Aberrant activity in the hippocampus "default pathway" is linked to cognitive decline in patients with AD (Buckner et al., 2005). By contrast, behavioral activation is reported to reduce plaque load in a mouse model of AD (Lazarov et al., 2005), and epidemiological studies suggest that cognitive activity is protective for AD (Cracchiolo et al., 2007). The absence of a molecular understanding of how activity increases Aβ accumulation has limited deeper appreciation of the contribution of activity to AD pathogenesis.

Our previous studies have focused on cellular immediate early genes (IEG) as potential mediators of protein synthesis dependent memory. Among them, Arc is a neuron-specific, postsynaptic protein that interacts with endophilin and dynamin and contributes to an endocytic pathway that accelerates removal of AMPA receptors from excitatory synapses (Chowdhury et al.,

2006). Arc is required for multiple forms of synaptic plasticity that depend on its endocytic function including homeostatic scaling (Shepherd et al., 2006) and mGluR-LTD (Park et al., 2008). Arc is an intriguing candidate that could participate in activity-dependent Aβ generation since endocytic pathways are important for regulation of BACE1 activity (Huse et al., 2000). Moreover, dominant-negative dynamin, which blocks endocytosis, reduces Aβ levels in ISF by as much as 70%, and prevents activity-dependent increases in Aβ (Cirrito et al., 2008).

Here, we report that Arc is required for activity-dependent increases of Aβ generation, and reveal a role for Arc in postsynaptic trafficking and processing of APP that appears relevant to the pathogenesis of AD. Arc directly binds the N terminus of PS1, the catalytic subunit of the γ-secretase complex, and these proteins colocalize in early/recycling endosomes within dendrites. Interruption of the Arc-PS1 interaction prevents activity-dependent increases of Aβ, and cell biological studies support a role for Arc in trafficking γ-secretase to vesicles that process APP. Arc-dependent Aβ generation contributes to plaque deposition in a mouse model of AD, and Arc expression is significantly elevated in the medial prefrontal cortex of patients with pathologically confirmed AD. Together, these findings demonstrate that Arc-dependent mechanisms, which are known to control synaptic strength, also control activity-dependent generation of Aβ that is relevant in the pathogenesis of AD.

RESULTS

Genetic Deletion of Arc Prevents Activity-Dependent Generation of Aβ

We crossed the amyloidogenic AD mouse model (*APPswe; PS1ΔE9* transgenic mice) to Arc KO ($Arc^{-/-}$) mice. The *APPswe; PS1ΔE9* mouse is an established model exhibiting accelerated Aβ amyloidosis attributable to coexpression of two familial AD linked mutations (hereafter referred to as AD mice) (Jankowsky et al., 2001). We first examined soluble hAβ levels in 5-month-old $AD;Arc^{+/+}$ and $AD;Arc^{-/-}$ mice. hAβ40 was not significantly different in hippocampus of $AD;Arc^{+/+}$ versus $AD;Arc^{-/-}$ mice sacrificed immediately upon removal from their home cage (Figure 1A). We used maximal electroconvulsive seizure (MECS) to acutely increase neural activity, and confirmed a ~2-fold increase of soluble hAβ40 5 hr after a single MECS in hippocampus from $AD;Arc^{+/+}$ mice (Figure 1A). By contrast, MECS did not increase soluble hAβ40 in hippocampus from $AD;Arc^{-/-}$ mice despite typical MECS behavioral responses and MECS-induced increase of IEG Homer1a (Figure 1A).

We examined acute brain slices prepared from 8- to 9-week-old $AD;Arc^{+/+}$ and $AD;Arc^{-/-}$ mice. Hippocampal slices were treated with picrotoxin (100 μM), which induces epileptiform activity by blocking GABAergic inhibition. Soluble hAβ40 increased during in vitro incubation, and basal levels were reliably detected after 10 hr incubation (Figure 1B). As reported (Kamenetz et al., 2003), picrotoxin treatment increased soluble hAβ40 in slices from *AD* mice (Figure 1B). By contrast, picrotoxin failed to increase soluble hAβ40 in slices from $AD;Arc^{-/-}$ mice.

We next examined DIV10 primary neuronal cultures prepared from $AD;Arc^{+/+}$ and $AD;Arc^{-/-}$ embryos. Soluble hAβ40 was assayed in whole cell lysates of neurons, or in the medium, 4 hr after a complete replacement with fresh glial conditioned medium (which was confirmed to have undetectable levels of Aβ, data not shown). >95% of soluble hAβ40 was present in the medium and only low levels were detected in neuronal lysates (Figure 1C); consistent with reports that Aβ is rapidly secreted after it is generated. In basal conditions, the level of hAβ40 was significantly less in the medium of $AD;Arc^{-/-}$ neuronal cultures compared to $AD;Arc^{+/+}$ cultures. Addition of picrotoxin (100 μM) for 4 hr, resulted in a significant increase of hAβ40 in medium of $AD;Arc^{+/+}$ neuronal cultures but not in medium of $AD;Arc^{-/-}$ cultures. BDNF (100 ng/ml for 4 hr) produced a prominent upregulation of Arc expression and resulted in an increase of hAβ40 in medium of $AD;Arc^{+/+}$ but not $AD;Arc^{-/-}$ cultures (Figure 1C). Lentiviral expression of Arc in $AD;Arc^{-/-}$ cultures resulted in an increase of soluble Aβ40 in the media compared to either uninfected or lentiviral-GFP infected $AD;Arc^{-/-}$ cultures. Thus, Arc transgene expression is sufficient to increase soluble Aβ40 generation in $AD;Arc^{-/-}$ neurons.

Arc Binds the N Terminus of PS1

We performed immunoprecipitation (IP) assays from WT and Arc KO brains using detergent conditions (1% Triton) that dissociate proteins in the γ-secretase complex. PS1-NTF selectively coimmunoprecipitated with Arc, while PS1-CTF, BACE1 and Nicastrin did not (Figure 2A). PS1-CTF and additional components of the γ-secretase, e.g., Nicastrin, co-IPed with Arc when the IP was performed using detergent conditions that retain interactions between components of γ-secretase (see Figure 6). In a reciprocal assay, Arc and PS1-CTF coimmunoprecipitated with PS1-NTF (Figure 2B). The physical interaction of Arc and PS1 was reconstituted in HEK293 cells using *PS1* and *Arc* transgenes (Figure 2C). PS1-NTF and full-length PS1 coimmunoprecipitated with full-length Arc or an N-terminal fragment of Arc (Arc 1–154). Deletion of Arc amino acids 91–100 or 101–130 disrupted Arc's association with PS1. Binding between Arc and PS1 was also reconstituted using recombinant Arc protein purified from *E. coli* together with Flag-PS1-NTF affinity purified from HEK293 cells (Figure 2D). This in vitro binding was selectively inhibited by a synthetic peptide mimic of the N-terminal 40 amino acids of PS1-NTF but not a peptide mimic of amino acids of 41–81 (Figure 2E). These observations suggest that Arc and PS1 directly and specifically interact.

Arc KO Does Not Alter Surface Expression of APP, BACE1, or γ-Secretase, or Their Trafficking from the Plasma Membrane

Current models of Aβ generation suggest that APP is processed by BACE1 and γ-secretase in early and recycling endosomes (Small and Gandy, 2006; Vetrivel and Thinakaran, 2006). We examined the possibility that Arc might increase Aβ generation by increasing the rate of endocytosis of APP, BACE1 or γ-secretase. DIV 14 cortical cultures were prepared from $AD;Arc^{+/+}$ and $AD;Arc^{-/-}$ embryos, and surface proteins were labeled by incubating cultures at 4°C with membrane-impermeable biotinylating reagent. Expression of APP, BACE1, and components of γ-secretase, including PS1 and Nicastrin, was not different between genotypes in either the total cell lysates or on the plasma

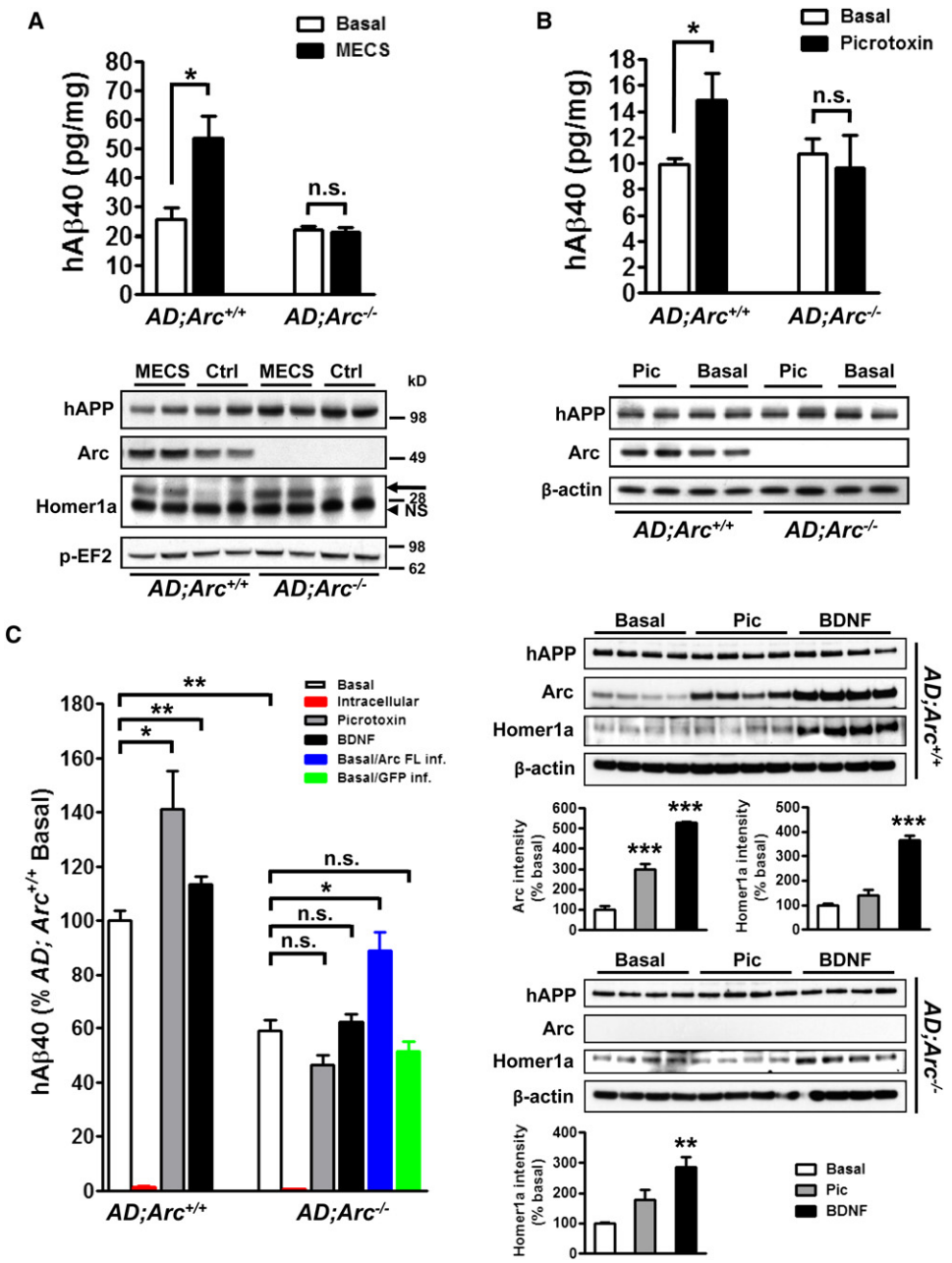

Figure 1. Genetic Deletion of Arc Abolishes Activity-Dependent Increases of hAβ40

(A) ELISA showing increase of PBS-soluble hAβ40 5 hr after MECS in hippocampus of *AD;Arc*$^{+/+}$ mice but not *AD;Arc*$^{-/-}$ mice. n = 4 for each group. *p < 0.05, two-tailed t test. Western blot confirms identical MECS-induced increase of Homer1a (arrow). Arrowhead with NS marks a nonspecific band.

(B) Picrotoxin increases soluble hAβ40 from acute brain slices of *AD;Arc*$^{+/+}$ mice, but not *AD;Arc*$^{-/-}$ mice. n = 10 per group. *p < 0.05, two-tailed t test. Western blot confirms hAPP was similarly expressed in brain slices of both genotypes.

(C) Picrotoxin and BDNF increase soluble hAβ40 in medium of cortical cultures from *AD;Arc*$^{+/+}$, but not *AD;Arc*$^{-/-}$ mice. Basal expression of hAβ40 is reduced in *AD;Arc*$^{-/-}$ cultures. Overexpression of Arc by lentivirus in *AD;Arc*$^{-/-}$ neurons increases hAβ40 production. n = 4–7 per group. *p < 0.05; **p < 0.01, two-tailed t test. Note that hAβ40 in cell lysates is < 5% of medium. Western blot confirms hAPP was similarly expressed under all conditions and Homer1a was similarly induced after BDNF in neuronal cultures of both genotypes. n = 4, **p < 0.01; ***p < 0.001, two-tailed t test.

Data represent mean ± SEM.

membrane (Figure 2F). PS1 NTF antibody detected both PS1ΔE9 transgene and a lower amount of processed native PS1 NTF, and this was not different in *AD;Arc*$^{-/-}$ neurons. The rate of endocytosis of surface-labeled APP and presenilin assayed 10, 30, and 60 min after return to 37°C was not different between genotypes (Figures S1A and S1B available online).

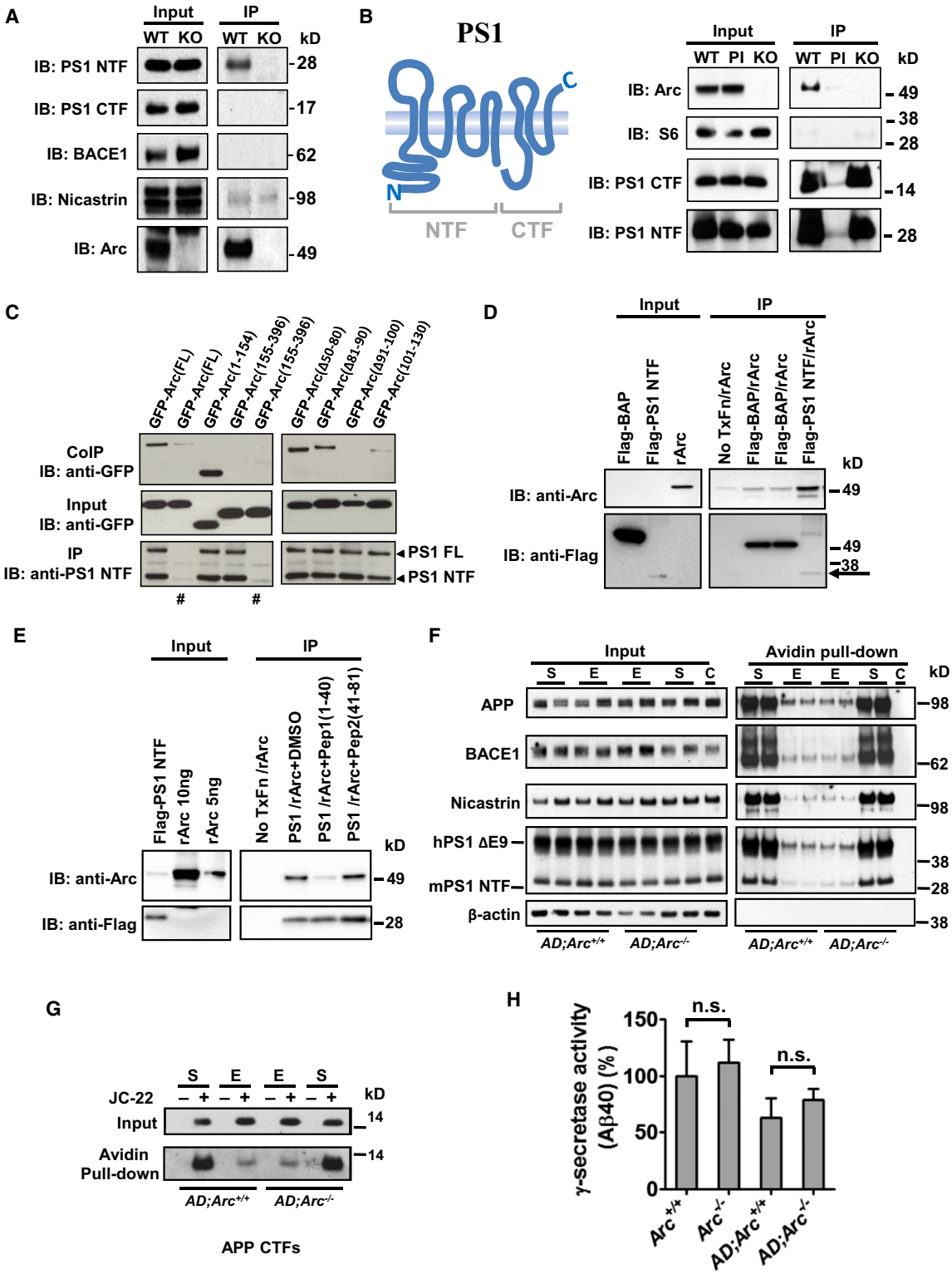

Figure 2. Arc Binds to Presenilin 1 N Terminus, and Arc Does Not Alter APP or Its Processing Enzymes Expression, Trafficking from the Plasma Membrane, or Activity

(A) Coimmunoprecipitation assay demonstrating association of endogenous PS1 with Arc. Anti-Arc antibody was used for immunoprecipitation (IP) from WT and Arc KO mouse brains, and immunoprecipitated proteins were blotted with anti-PS1 NTF, PS1 CTF, BACE1, or Nicastrin antibody. PS1 NTF selectively coimmunoprecipitates with Arc.

Treatment of cultured neurons with the selective γ-secretase inhibitor JC-22 (Lewis et al., 2005) resulted in identical increases of C-terminal fragments of APP that result from cleavage by BACE1 and/or α-secretase (Figure 2G), suggesting that APP processing upstream of γ-cleavage is not different in neurons derived from *AD;Arc*$^{+/+}$ and *AD;Arc*$^{-/-}$ mice. An in vitro assay of γ-secretase activity measured from forebrain lysates, using biotinylated recombinant APP substrate Sb4 (Shelton et al., 2009) in the presence of 0.25% CHAPSO, did not detect an effect of Arc in comparisons of *Arc*$^{+/+}$ versus *Arc*$^{-/-}$ or *AD;Arc*$^{+/+}$ versus *AD;Arc*$^{-/-}$ mice in terms of production of Aβ40 peptides using a G2-10 antibody (Tian et al., 2010) (Figure 2H). Thus, the effect of Arc increasing Aβ40 generation in cultures could not be related to altered dynamics of APP, BACE1, or γ-secretase trafficking from the plasma membrane, or to prominent changes in either BACE1 or γ-secretase expression or activity.

Arc and PS1 Colocalize in Postsynaptic Dendrites in Association with Endosome Membranes

Biochemical and electron microscopic (EM) methods indicate that Arc protein is present exclusively in the postsynaptic compartment (Chowdhury et al., 2006). EM studies have reported APP and PS1 in both pre- and postsynaptic compartments (Ribaut-Barassin et al., 2000). We detected native PS1 in dendrites (Figure 3A) using an antibody with confirmed specificity for immunostaining (Figure S1C). Coexpression of *Arc* and *PS1* transgenes in DIV14 neurons resulted in colocalizing punctae in dendrites (Figure 3B), especially in fine processes where punctae are discrete (technical note: low-power images that indicate the position of the processes typically appear overexposed at regions of the neuron including the soma and proximal dendritic branches as a consequence of their greater thickness). Colocalization required coexpression of endophilin 3, which enhances Arc association with endosomes (Chowdhury et al., 2006). To determine whether the Arc-PS1 punctae were endosomes, we examined the colocalization of Arc-PS1 punctae with endosomal markers. In neurons expressing *GFP-Rab11*, a recycling endosome marker, we could detect the colocalization between Arc, PS1, and Rab11 (Figure 3C). Costes' method (Costes et al., 2004) was applied to evaluate the probability of colocalization between Arc and PS1, or PS1 and Rab11 (Figure 3C, probability graph). The Pearson's coefficient of double-channel images (PS1 and Arc, or PS1 and Rab11) confirms a high probability of colocalization (Figure 3D, scatter plot). Quantitative analysis revealed prominent colocalization of Arc with PS1(45.0 ± 3.0%), Arc with EEA1 (26.3 ± 3.4%) and Rab11 (50.0 ± 4.4%), and PS1 with EEA1 (23.5 ± 3.6%) and Rab11 (43.3 ± 4.5%) (Figure 3D, table). EM analysis of normal rat hippocampus revealed that native PS1 and native Arc colocalize in postsynaptic spines of CA1 neurons (Figures 3E and 3F). Gold particles are associated with vesicles immediately beneath the postsynaptic density as well as with structures identified as early/recycling endosomes based on their tubulovesicular structures (Figures 3G–3P). Several profiles of endosomal complex structures extending from the sorting/early endosome (oval, spindly vesiculate shape) are labeled with Arc and PS1 (Figures 3G–3L, 3N, and 3O). Double EM also revealed colocalization of PS1 with Rab11 (Figures 3M and 3P).

APP Is Rapidly Internalized in Postsynaptic Early/Recycling Endosomes that Associate with Arc

We examined trafficking of APP in dendrites of DIV14 neurons prepared from *AD;Arc*$^{+/+}$ mice. Neurons were fixed and stained

(B) Schematic representation of PS1 structure and coimmunoprecipitation assay demonstrating association of endogenous Arc with PS1. Anti-PS1 NTF antibody or preimmune serum was used for IP from WT and Arc KO mouse brains, and immunoprecipitated proteins were blotted with anti-Arc, PS1 CTF or S6 antibody. Arc and PS1 CTF coimmunoprecipitate with PS1 NTF.

(C) Endogenous PS1 coimmunoprecipitates with GFP-Arc from HEK293 cells. Anti-PS1 NTF antibody and preimmune serum (#) were used for IP. Precipitated proteins were blotted with anti-GFP antibody. PS1-NTF and full-length PS1 coimmunoprecipitate with full-length Arc, and with an N-terminal fragment of Arc (Arc 1–154). Deletion of Arc amino acids 91–100 or 101–130 prevents Arc's association with PS1.

(D) In vitro binding assay demonstrates that recombinant Arc protein (rArc), purified from *E. coli*, binds to Flag-PS1 NTF that was overexpressed and affinity-purified from HEK293 cells. Flag-BAP (BRCA1 Associated Protein) and cell lysate from HEK293 cells without transfection (NoTxFn) were used as controls for binding assay. The first three lanes are loading controls for Flag-BAP, Flag-PS1 NTF, and rArc. The remaining four lanes are the coimmunoprecipitated samples using Protein G beads bound with Flag antibody. An arrow denotes Flag-PS1 NTF in the anti-Flag immunoblot.

(E) The first three lanes show loading controls for Flag-PS1 NTF, 10 ng and 5 ng of rArc. The remaining four lanes are the coimmunoprecipitated samples, showing no binding of rArc with an untransfected cell extract, a preferential binding of rArc with Flag-PS1 NTF expressing cell extract in the presence of DMSO (a control for the peptides, which were dissolved in DMSO), a selective inhibition of binding between rArc and PS1 NTF by Peptide 1(1–40), and no inhibition by Peptide 2(41–81).

(F) Surface expression (S) and endocytosis (E) of APP, BACE1 and components of γ-secretase from cortical cultures are not different between *AD;Arc*$^{+/+}$ and *AD;Arc*$^{-/-}$. Surface proteins were labeled at 4°C with 1mg/mL EZ-Link Sulfo-NHS-SS-Biotin and total cell lysates (Input, left) were affinity enriched for surface proteins by NeutrAvidin pull-down (right). Protein endocytosis was similarly assayed 30 min after return of surface-labeled neurons to 37°C, and the remaining surface bound biotin was removed by 150 mM glutathione-stripping buffer (pH 8.6–8.7). Control cultures (C) were surface biotinylated and stripped without endocytosis. Lysates (Input) and avidin pulldown elutes (surface or endocytosed proteins) were analyzed by western blot. Detailed time course data is presented in Figure S1A and Figure S1B.

(G) APP CTFs increase following treatment of cortical cultures with γ-secretase inhibitor JC-22 for 48 hr. Surface biotinylation and endocytosis assays showing that surface expression (S) or endocytosis (E) of APP CTFs is not different between *AD;Arc*$^{+/+}$ and *AD;Arc*$^{-/-}$.

(H) γ-secretase activity in forebrain lysates measured in vitro using the recombinant substrate Sb4 is not different between *Arc*$^{+/+}$ and *Arc*$^{-/-}$ or between *AD;Arc*$^{+/+}$ and *AD;Arc*$^{-/-}$ mice. Data represent mean ± SEM (n = 4–5 per group). The γ-secretase mediated cleavage is monitored by G2-10 antibody that specifically recognizes the C terminus of Aβ40, but not the substrate. The assay background or nonspecific cleavage was defined in the presence of 1 μM γ-secretase inhibitor L685, 458.

See also Figure S1.

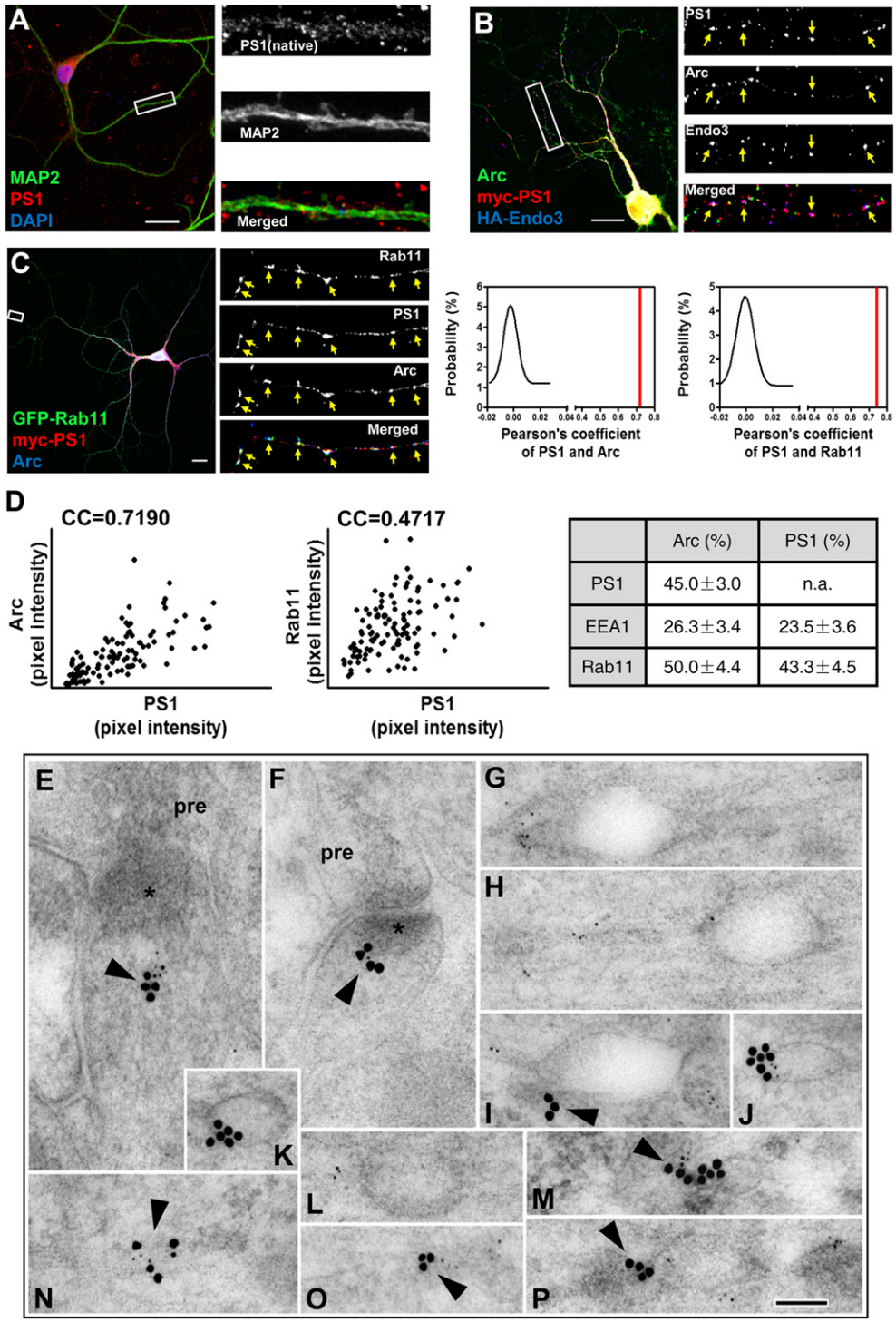

	Arc (%)	PS1 (%)
PS1	45.0±3.0	n.a.
EEA1	26.3±3.4	23.5±3.6
Rab11	50.0±4.4	43.3±4.5

Figure 3. Arc and Presenilin1 Colocalize in Endosomes in Neuronal Dendrites

(A) Representative image from WT mouse hippocampal neuron showing native PS1 localizes in neuronal dendrites identified by MAP2 staining.

(B) Representative image from WT rat hippocampal neuron transiently transfected with *Myc-PS1*, *Arc* and *HA-Endophilin 3(Endo3)*. PS1 colocalizes with Arc and Endophilin3 puncta in neuronal dendrites.

(C) Representative image of WT hippocampal neuron expressing Arc, HA-Endo3, Myc-PS1 and GFP-Rab11. Arc and PS1 partially colocalize with Rab11 in neuronal dendrites indicated by yellow arrows. Plot of the probability distribution of Pearson's coefficients of randomized images (curve) and of the Pearson's coefficient of double-channel images (red line; PS1 and Arc, or PS1 and Rab11). Note that the p value for this analysis was 100% indicating a high probability of colocalization.

with 6E10 monoclonal antibody, which reacts with the Aβ sequence present in hAPP. Staining was present along dendrites that costained with MAP2 (Figure 4A). A similar pattern of staining was detected with two additional APP antibodies: 22C11, which reacts with the N terminus of human or mouse APP (Figure S1D), and 4G8, which reacts with the Aβ epitope in both human and mouse APP (data not shown). By incubating live neurons from *AD;Arc*$^{+/+}$ with 6E10 at 10°C, and then returning the neurons to 37°C for 10 min, we could detect hAPP internalized into dendrites (Figure 4B). The same result was obtained with 22C11 (Figure S1E). hAPP labeled on the surface by 6E10 was internalized into punctae that colocalized with Rab11 (Figure 4C), suggesting APP is trafficked in recycling endosomes. Consistent with dendritic localization, APP, PS1ΔE9, and Arc are enriched in biochemical fractions of the postsynaptic density (Figure 4D). EM analysis of normal rat hippocampus with two different APP antibodies verified the presence of APP in postsynaptic vesicles near the PSD, and in endosomal complexes composed of different tubulovesicular structures (Figures 4E–4N, 4G8 antibody; Figures S1F–S1K, 22C11 antibody). Double EM revealed colocalization of APP with Arc (Figures 4E–4G, 4I–4K, 4M, and 4N; Figures S1G–S1J), and Arc with Rab11 (Figure S2A-G) at endosomes. Quantitative analysis of immunogold labeling of dendrites demonstrated a substantial amount of Arc, PS1 and APP are associated with tubulovesicular structures (Figure 4O). Additionally, Arc, endophilin3 and dynamin cofractionate with PS1 and APP-CTF in detergent-resistant, buoyant fractions (lipid raft) prepared from *AD;Arc*$^{+/+}$ mice that are enriched for proteins that process APP (Vetrivel et al., 2005) (Figure S2H). This distribution was not altered in *AD;Arc*$^{-/-}$ mice (Figure S2I).

Arc Increases Association of γ-Secretase with APP Containing Endosomes

Transiently expressed hAPP was labeled on the dendritic surface with 6E10 monoclonal antibody (Figure S3A), and endocytosed hAPP was detected as bright, discrete punctae in both dendrites and axons (Figures S3C and S3D), consistent with endogenous APP. Identical results were observed with wild-type hAPP and hAPPswe (data not shown). In comparison to natively expressed hAPP, hAPP transgene could be detected with direct conjugated secondary antibody, and could be easily assessed for colocalization with other proteins. When hAPP transgene was coexpressed with Arc, endophilin3 and GFP-Rab11, surface-labeled hAPP rapidly internalized into dendrites and colocalized with Arc and Rab 11 (Figure 5A). Evaluation of colocalization by Costes' approach revealed a high probability of colocalization between internalized APP and Arc, or internalized APP and Rab11 (Figure 5A, graph). Quantitative analysis further demonstrated the positive correlation (Figure 5B, scatter plot) and a significant population of colocalized APP (internalized) and Arc is present in endosomes and with higher percentage in recycling endosomes [Figure 5B and Figure S4A, 33.6 ± 4.3%, 28.4 ± 1.7% and 45.8 ± 3.7%, respectively, for early (Rab5^{+}), late (Rab7^{+}) and recycling (Rab11^{+}) endosomes]. ~50% of internalized hAPP colocalized with Arc (Figures S3E and S3F). Another early/recycling endosome marker, transferrin receptor, also colocalized with Arc and internalized hAPP (Figure S4B). hAPPswe was similarly internalized and colocalized with transferrin receptor (Figure S4C). Association between internalized APP and early or recycling endosomes was further confirmed by live confocal imaging using GFP-Rab5 or Rab11 and Alexa 568-labeled APP antibody (Figure S4D). These observations support the hypothesis that APP is trafficked in dendritic early/recycling endosomes that associate with Arc.

A similar approach was used to monitor trafficking of BACE1. HA-BACE1 was detected on the neuronal surface by live labeling with HA antibody (Figure S3B), and was rapidly internalized into dendrites where it colocalized with Arc-endophilin punctae (Figure 5C).

To examine the possibility that Arc might regulate the association of APP with γ-secretase, we expressed *hAPP* transgene in *Arc*$^{+/+}$ and *Arc*$^{-/-}$ neurons and assessed colocalization with native PS1. hAPP was labeled on the membrane with 6E10 and internalized following a 10 min return to 37°C. hAPP was identically internalized in *Arc*$^{+/+}$ and *Arc*$^{-/-}$ neurons (Figure 5E), consistent with biochemical assays of native APP (Figure 2F and Figure S1A). PS1 particle number in randomly selected 50 μm dendritic segments was not different between *Arc*$^{+/+}$ and *Arc*$^{-/-}$ neurons (Figure S5). Internalized hAPP punctae frequently colocalized with PS1 punctae (Figure 5D). Costes' method revealed a high probability of colocalization (data not shown). We quantitatively compared the degree of colocalization of internalized hAPP with native PS1 in randomly selected 50 μm dendritic segments. Colocalization of PS1 with APP containing vesicles was significantly greater in *Arc*$^{+/+}$ than *Arc*$^{-/-}$ neurons (Figure 5F). This finding supports a model in which Arc functions to increase γ-secretase in dendritic trafficking endosomes that process APP.

(D) Scatter plot of pixel intensity correlations between PS1 and Arc, or PS1 and Rab11 in hippocampal neurons represented by (C). Correlation coefficients (CC) are shown. The percentage of Arc-positive or Myc-PS1-positive pixels overlapping with Myc-PS1, endogenous EEA1 or GFP-Rab11 was quantified by Imaris software (Bitplane). Data represent mean ± SEM (n = 15–35).

Images in (A)–(C) are representative of 3 independent experiments and at least five imaged neurons; scale bars represent 20 μm. See also Figure S1.

(E–P) Postembedding immunogold localization (arrowheads) of Arc, Presenilin 1 and Rab11 in endosomes in the adult rat hippocampus (two animals) in postsynaptic spines ([E and F]; E is oblique), large, apical pyramidal cell dendrites (G, H, L, M, and N) and soma (I and J). Double immunogold labeling includes Presenilin (5 nm) + Arc (15 nm; E–L, N, O), and Presenilin1 (5 nm) + Rab11 (15 nm; [M and P]). Micrographs of dendrites are oriented with the long axis from left to right. Labeled recycling endosomes can sometimes be traced directly back to their origin as outgrowths from large oval sorting/early endosomes (G, H, I, and L). Distinct colocalization of Arc and PS1 within a gold cluster is illustrated as in (E), (F), (J), (N), and (O). Other micrographs illustrate colocalization within the same endosome or endosomal complex for Arc+PS1 (I), and PS1+Rab11 (M and P). Micrographs were taken from the CA1 stratum radiatum (E–H, N, and O) or stratum pyramidale (I and M), CA2 stratum radiatum (K and P) or CA3 stratum lucidum (J and L). pre, presynaptic terminal; asterisk, postsynaptic density.

Scale bar in E–P is 100 nm.

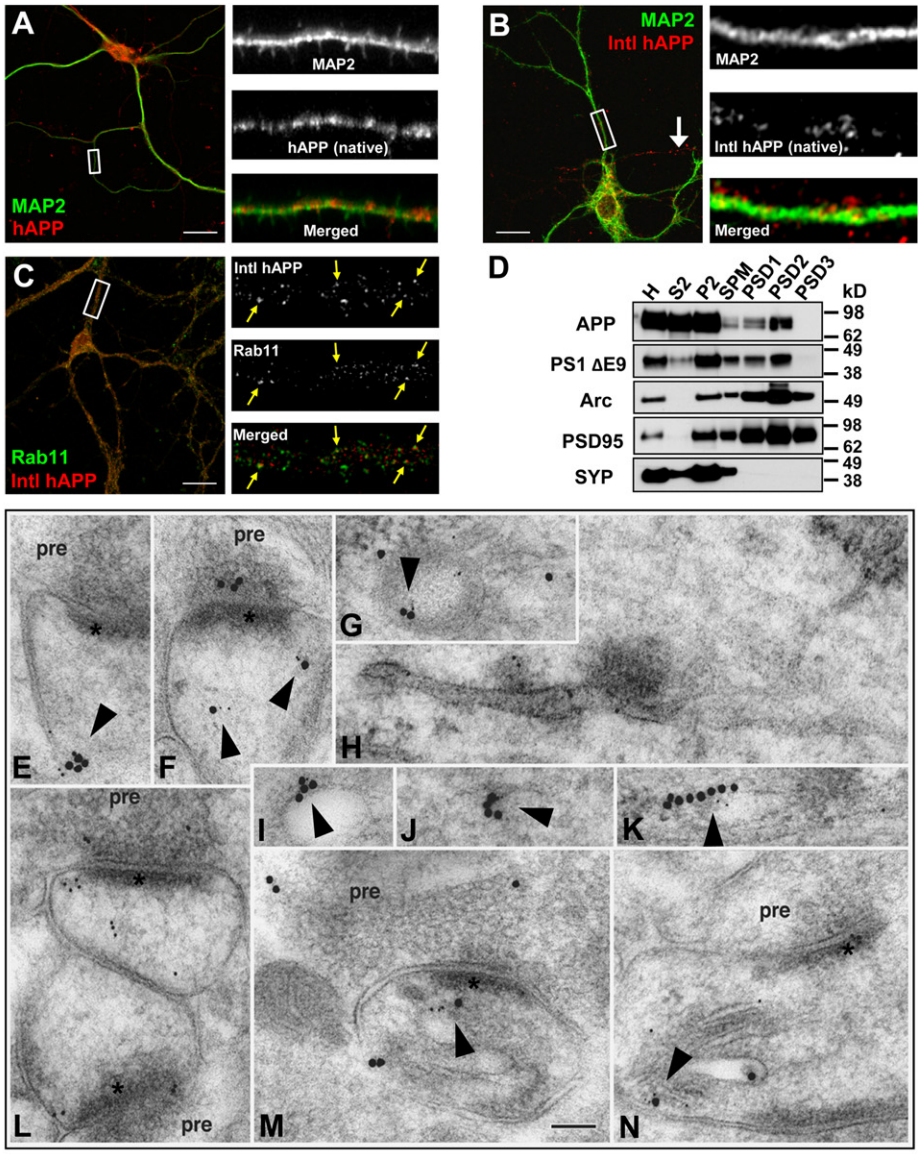

O

		Arc	PS1	APP	Control 1	Control 2
Postsynaptic Spine (gold/spine)		1.50±0.17	0.32±0.06	1.80±0.20	0.01±0.01	0.01±0.01
Dendrite (gold μm^{-2})	total gold	9.36±0.73	2.95±0.26	17.33±0.99	0.08±0.03	0.21±0.06
	T-V organelle -associated	5.37±0.56	2.30±0.23	10.03±0.62	0.05±0.02	0.15±0.05
% of total gold in T-V organelle		56.36±1.77	77.52±4.05	59.09±2.61	n.a.	n.a.

Figure 4. APP Is Rapidly Internalized into Endosomes in Neuronal Dendrites and Associates with Arc

(A) Representative image from *AD;Arc*$^{+/+}$ hippocampal neurons showing that natively expressed hAPP localizes in neuronal dendrites identified by MAP2 staining. (B and C) Representative images from endocytosis assay and double-immunofluorescence labeling of *AD;Arc*$^{+/+}$ hippocampal neurons showing natively expressed hAPP that is labeled on the cell surface with 6E10 antibody is rapidly internalized into dendrites, identified by MAP2 staining (B), and colocalizes with native Rab11 (C). White arrow in panel (B) points to a probable axon where hAPP is also internalized.

Images in (A)–(C) are representative of three independent experiments and at least five imaged neurons; scale bars represent 20 μm.

(D) Subcellular fractionation of adult *AD;Arc*$^{+/+}$ mouse forebrain showing APP, Presenilin1 and Arc localize in postsynaptic densities (PSD1-3). H, homogenate; S2, supernatant, cytosolic fraction; P2, crude synaptosomal fraction; SPM, synaptosomal plasma membrane; PSD1, 1 Triton solubilized SPM; PSD2, 2 Triton solubilized SPM; PSD3, Triton and Sarkosyl solubilized SPM; SYP, synaptophysin.

Interruption of Arc Association with γ-Secretase Prevents Activity-Dependent Increase of Aβ Generation

To further examine the role of Arc binding to PS1 in the generation of Aβ, we generated lentivirus expressing Flag-tagged PS1 NTF and confirmed that Flag-PS1 NTF coimmunoprecipitates with Arc from neurons (Figure 6A). A previous study reported that PS1-NTF does not integrate into γ-secretase (Levitan et al., 2001), and we confirmed that Flag-PS1 NTF does not associate with components of the native γ-secretase complex in neurons (Figure 6B). Using lysates prepared from neurons and detergent conditions that do not disrupt the γ-secretase complex (Capell et al., 1998), Arc coimmunoprecipitated PS1-CTF and Nicastrin (indicators of its association with the γ-secretase complex), and this association was interrupted by Flag-PS1 NTF (Figure 6C). Importantly, expression of Flag-PS1 NTF in *AD;Arc*$^{+/+}$ neurons blocked the activity-dependent increase of Aβ40 (Figure 6D). Flag-PS1 NTF also produced a modest reduction of basal Aβ in *AD;Arc*$^{+/+}$ neurons. By contrast, Flag-PS1 NTF did not alter basal or induced expression of Aβ40 in *AD;Arc*$^{-/-}$ cultures indicating that Flag-PS1 NTF does not alter γ-secretase activity in neurons that lack Arc.

Aβ and Plaque Load Are Reduced in *AD;Arc*$^{-/-}$ Mice

We next determined if Arc contributes to amyloid generation and deposition in vivo. The *APP*$_{SWE}$*;PS1ΔE9* model shows an age-dependent increase of PBS-soluble and PBS-insoluble (formic acid-soluble) hAβ together with demonstrable plaque in cortex by 6 months of age. Genetic crosses of *AD;Arc*$^{+/-}$ with Arc$^{+/-}$ assured that all mice carried a single copy of the *APPswe and PS1ΔE9* transgene, and provided littermate controls. Western blots confirmed that expression of native mouse APP and human APPswe was identical in forebrain of *AD;Arc*$^{+/+}$ versus *AD;Arc*$^{-/-}$ mice (Figure S6A). Similarly, expression of BACE1 and components of γ-secretase complex were not different between genotypes (Figure S6A). However, in 6-month-old male mice, the amount of Aβ40 in a formic acid soluble fraction was reduced in *AD;Arc*$^{-/-}$ mice. Aβ42 showed the same trend but was not statistically different between genotypes (Figure 7A). In 12-month-old mice, both Aβ40 and Aβ42 levels were reduced in *AD;Arc*$^{-/-}$ versus *AD;Arc*$^{+/+}$ male (Figure 7B) and female mice (Figure S6B). Immunohistochemistry in cohorts of 6-month-old male (Figures 7C and 7D) and 12-month-old female mice (Figures S6C and S6D) confirmed that areas occupied by Aβ plaque were reduced in *AD;Arc*$^{-/-}$. These results suggest that Arc contributes significantly to amyloid burden in this AD model.

Arc Expression Is Increased in Medial Frontal Cortex of Patients with Alzheimer's Disease

To further explore the role of Arc in AD, we compared expression of Arc protein in gray matter punch samples from medial frontal cortex (MFC) or occipital cortex (OCC) of autopsies of patients with dementia that was highly likely due to AD based on the presence of both neuritic plaque and neurofibrillary tangles in neocortex (CERAD C and Braak Stage V and VI) and patients with intermediate likelihood that dementia was due to AD based on neuritic plaque in neocortex and neurofibrillary tangles in limbic regions (CERAD B and Braak Stage III and IV) versus samples from age matched controls (patient data is summarized in Table S1). MFC and OCC were selected because MFC is commonly impacted in AD and used in both CERAD and Braak Staging as representative neocortex, while OCC (primary visual area) is not a major brain region impacted in AD. Levels of Arc protein in MFC were increased in the combined AD group compared to the control group (Figures 7E and 7F and Figure S7A) by ~2 fold. Arc levels were not significantly different between the high likelihood versus intermediate likelihood AD cases. Zif268, an IEG that shows similar response as Arc to activity, was not different between AD and control brains. Levels of Arc or Zif268 protein in OCC were not different between AD and control brains. While there are important limitations of post mortem tissue, the present data suggest that Arc expression is maintained at normal or supranormal levels in a brain area impacted by AD, and thus could contribute to Aβ generation and pathology.

DISCUSSION

The present study demonstrates that Arc is required for activity-dependent increases of Aβ, APP is trafficked in the dendritic compartment, and associates with Arc in early and recycling endosomes that presumably return processed APP as Aβ to the extracellular space where it accumulates. Arc also associates with presenilin in dendritic vesicular structures that include early endosomes and recycling endosomes. Arc directly binds the N terminus of PS1, and interruption of the interaction blocks activity-dependent increases of Aβ generation. Importantly, inhibitory effects of Flag-PS1 NTF on Aβ generation are evident only in neurons that express Arc, and γ-secretase activity is not different in Arc KO brain, suggesting that Arc does not directly modify the activity of γ-secretase. Rather, Arc increases the association of PS1/γ-secretase with endosomes that traffic APP. The catalytic site of the γ-secretase complex is present

(E–N) Postembedding immunogold localization of native Arc and APP in the adult rat hippocampus (two animals) in postsynaptic spines (E, F, and L), thorny excrescences ([M and N]; i.e., the enlarged spine-like structures postsynaptic to mossy terminals), and large, apical pyramidaly cell dendrites (G–K), labeled either singly for APP ([H and L]; 10 nm gold) or double-labeled (E–G, I–K, M, and N) for Arc (5 nm gold) and APP (15 nm gold). Micrographs of dendrites are oriented with the long axis from left to right; labeling is evident in tubulovesicular endosomal structures (H, J, and K) including some large sorting/early endosomes (G and I). Labeling in thorny excrescences is evident in tubulovesicular complexes. Colocalization of Arc and APP can be seen in both dendrites and postsynaptic structures (arrowheads). APP is also evident in presynaptic terminals (pre; [F, L, and M]). Micrographs were taken from the CA1 stratum radiatum (E–J and L) or CA3 stratum lucidum (K, M, and N). Asterisk, postsynaptic density. Scale bar is 100 nm.

(O) Table of postembedding immunogold localization of Arc, PS1, APP, and corresponding rabbit (control 1) and mouse (control 2) antibody controls, in adult rat hippocampus (2 animals; 10 nm gold; CA1 stratum radiatum). Labeling was counted in postsynaptic spines or in dendrites. Control values were subtracted from original values of Arc, PS1 and APP, to obtain values shown in table (mean ± SEM). Total number of spine synapses counted was 111, 164, 121, 170, 163 for Arc, PS1, APP, and controls 1 and 2, respectively. For dendrites, labeling of various tubulovesicular (T-V) organelles is a subset of the total labeling; for each antibody, dendrite profiles were measured in 30 micrographs (mean total of 92.46 μm^2 per antibody).

See also Figure S1 and Figure S2.

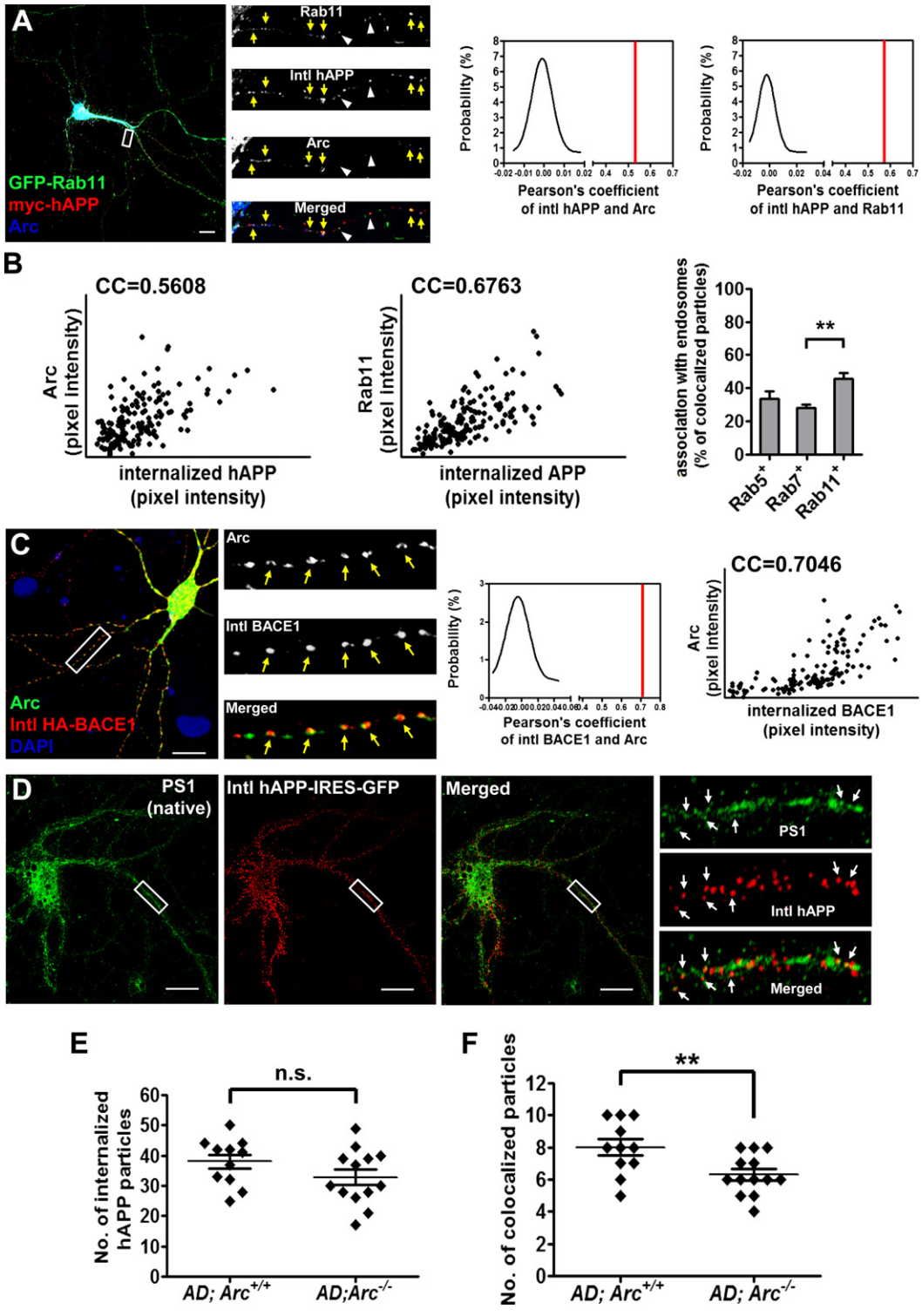

Figure 5. Trafficking Assays; Native Arc Enhances Association of Native γ-Secretase with hAPP Transgene Containing Endosomes

(A) Representative image from endocytosis assay and immunofluorescence labeling of WT hippocampal neurons transiently transfected with *Myc-hAPP*, *Arc*, *HA-Endo3*, and *GFP-Rab11* showing hAPP that is labeled on the cell surface with 6E10 antibody and rapidly internalized, colocalizes with Arc and GFP-Rab11 (yellow arrow). White arrowhead points to punctae with overlapped intl hAPP and Rab11 but not Arc. Plot of the probability distribution of Pearson's coefficients of randomized images (curve) and of the Pearson's coefficient of double-channel images (red line; internalized hAPP and Arc, or internalized hAPP and Rab11). Note that the p value for this analysis was 100% indicating a high probability of colocalization.

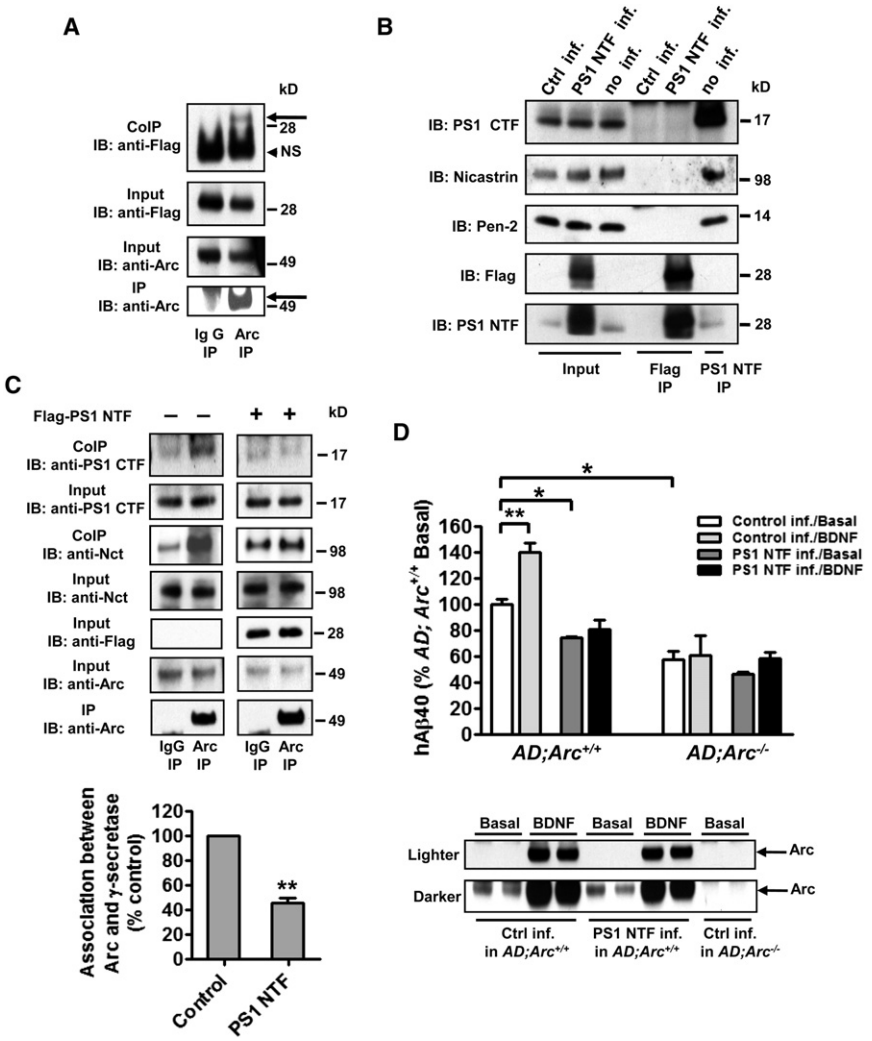

Figure 6. Interruption of Arc Binding to γ-Secretase Prevents Activity-Dependent Aβ Generation

(A) Lentivirus-expressed Flag-PS1 NTF coimmunoprecipitates with native Arc from cortical cultures. Anti-Arc antibody and mouse IgG were used for IP, and precipitated proteins were blotted with anti-Flag antibody. Arrows indicate bands for Arc and Flag-PS1 NTF. Dark, nonspecific bands (NS, indicated by arrowhead) are reactions to antibodies used for IP.

(B) Coimmunoprecipitation and western blots showing lenvirus-expressed Flag-PS1 NTF does not associate with components of the native γ-secretase complex. Anti-Flag antibody or anti-PS1 NTF antibody was used for IP from *Arc*$^{+/+}$ neurons infected with Flag-PS1 NTF lentivirus, control lentivirus expressing Flag-PS1 NTF in a reversed orientation, or without infection. Precipitated proteins were detected by immunoblot with anti-PS1 CTF, Nicastrin or Pen2 antibody. Only native PS1 NTF was able to coimmunoprecipitate PS1 CTF, Nicastrin, and Pen2.

(C) Coimmunoprecipitation and western blot assay showing Flag-PS1 NTF interrupts association between Arc and γ-secretase. Anti-Arc antibody or mouse IgG were used for IP from *Arc*$^{+/+}$ neurons infected with Flag-PS1 NTF lentivirus, or without infection. Precipitated proteins were blotted with anti-PS1 CTF antibody or anti-Nicastrin antibody as indicators of the associated γ-secretase complex. PS1 CTF and Nicastrin coimmunoprecipitate with Arc from noninfected neurons, and they are reduced in neurons expressing Flag-PS1 NTF. Quantification of coimmunoprecipitated PS1 CTF by densitometry indicated association between Arc and γ-secretase was significantly lower in neurons with Flag-PS1 NTF expression. n = 3 per condition from three independent experiments. **p < 0.01, two-tailed t test.

(D) Flag-PS1 NTF blocks activity-dependent increase of hAβ40 by BDNF in cortical cultures of *AD;Arc*$^{+/+}$ mice. Flag-PS1 NTF also reduces basal hAβ40 in *AD;Arc*$^{+/+}$ mice but does not alter basal or stimulated hAβ40 from *AD;Arc*$^{-/-}$ neurons. n = 4 per group. *p < 0.05, **p < 0.01, two-tailed t test. Western blot confirmed similar expression of Arc in control virus infected versus Flag-PS1 NTF infected neurons under basal condition or after BDNF activation. Data represent mean ± SEM.

within the transmembrane domain, and this mandates that its substrate be present in the same membrane. Since APP is present in the plasma membrane, along with BACE1 and low levels of components of γ-secretase, Arc could function to increase γ-secretase recruitment from the plasma membrane to the same endosome as APP and BACE1. However, we do

(B) Scatter plot of pixel intensity correlations between internalized hAPP and Arc, or internalized hAPP and Rab11 in hippocampal neurons represented by (A). Correlation coefficients (CC) are shown. The percentage of colocalized hAPP (internalized) and Arc puncta overlapping with Rab-positive puncta was also quantified. Data represent mean ± SEM (n = 8–15, **p < 0.01, ANOVA with Turkey post hoc test).

(C) Representative image from endocytosis assay and immunofluorescence labeling of WT hippocampal neurons transiently transfected with *HA-BACE1*, *Arc* and *Myc-Endo3* showing HA-BACE1 that is labeled on the cell surface, is internalized into dendrites, and colocalizes with Arc. Plot of the probability distribution of Pearson's coefficients of randomized images (curve) and of the Pearson's coefficient of double-channel images (red line; internalized BACE1 and Arc). Scatter plot of pixel intensity correlations between internalized hAPP and Arc. Correlation coefficient (CC) is shown.

(D) Representative image from endocytosis assay and immunofluorescence labeling of DIV21 WT mouse cortical neurons infected with hAPP-IRES-GFP Sindbis pseudovirus showing colocalization of hAPP that is labeled on the cell surface with 6E10 antibody and rapidly internalized (37°C, 10 min) with native PS1 in dendrites. In contrast to the extensive colocalization of internalized hAPP with Arc (A), only a portion of internalized hAPP colocalizes with PS1.

(E and F) Quantitative analysis of (D). The number of APP punctae labeled on the cell surface with 6E10 antibody and rapidly internalized (37°C, 10 min) was not different between genotypes (E), however colocalization of hAPP punctae with native PS1 was greater in *Arc*$^{+/+}$ than *Arc*$^{-/-}$ neurons (F). Data represent mean ± SEM (n = 11–13, **p < 0.01, two-tailed t test). Assays were performed on randomly selected 50 μm segments of dendrites from at least five cells for each genotype. Scale bars represent 20 μm. See also Figure S3, Figure S4, and Figure S5 for validation of trafficking assays.

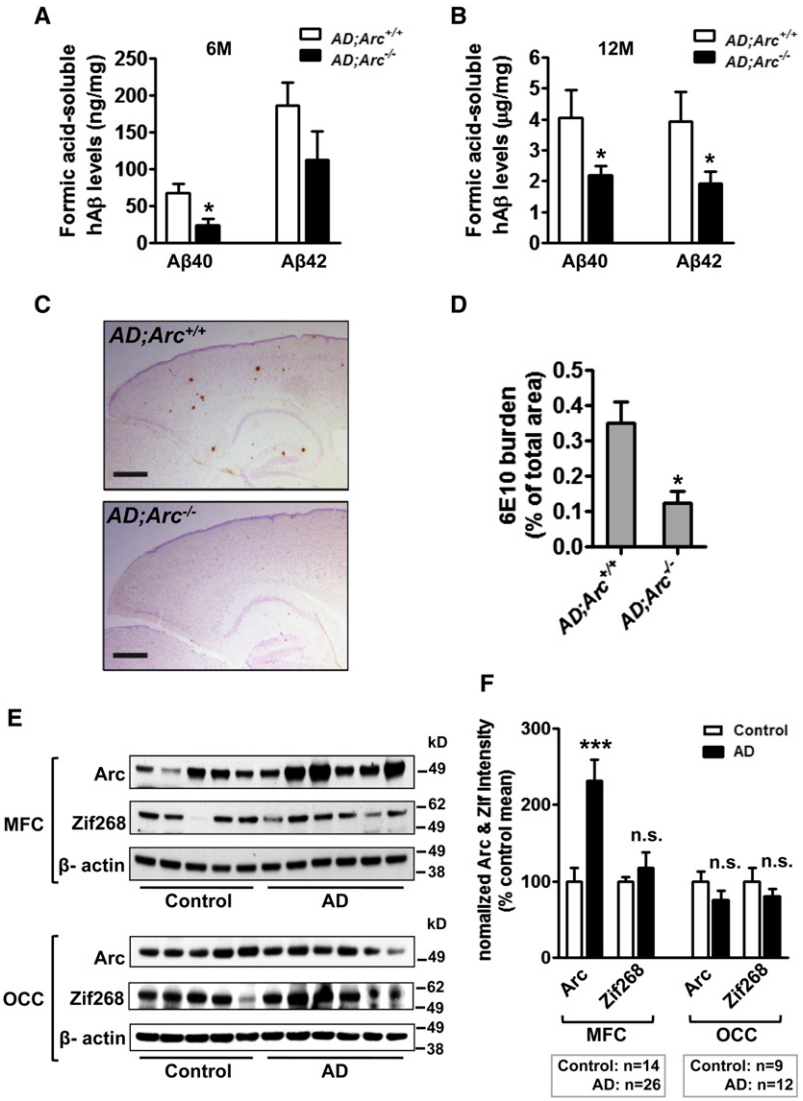

Figure 7. Arc Contributes to Aβ Levels and Plaque Load in *AD* Mice, and Is Elevated in Medial Frontal Cortex of Patients with Alzheimer's Disease

(A and B) ELISA showing reduction of formic acid-soluble hAβ levels in the forebrains of age-matched male *AD;Arc*$^{-/-}$ mice compared to *AD;Arc*$^{+/+}$ mice at 6 months (A) or 12 months (B) of age. n = 5–6 per genotype. *p < 0.05, two-tailed t test.

(C) Representative images show plaque load in the cortex of male mice at 6 months of age. Scale bars represent 250 μm.

(D) Analysis of plaque area in 6-month-old male mice demonstrating a reduction in *AD;Arc*$^{-/-}$ compared to *AD;Arc*$^{+/+}$ mice. n = 5–6 per genotype. *p < 0.016, Mann-Whiteney U test.

(E and F) Representative western blots (E) and quantification (F) indicating the expression of Arc is increased in samples of gray matter from medial frontal cortex of brains from AD patients compared to age-matched controls, while the expression of Zif268 is not different. Neither Arc nor Zif268 is different between control and AD patients in the occipital cortex. β-actin used as a loading control. ***p < 0.001, two-tailed t test. MFC, medial frontal cortex; OCC, occipital cotex. Control: n = 14 (MFC), n = 9 (OCC); AD patients: n = 26 (MFC), n = 12 (OCC).

Data represent mean ± SEM. See also Figure S6, Figure S7, and Table S1.

not detect an Arc-dependent change in the rate of internalization of γ-secretase, as might be expected in such a model. Consequently, we favor a model in which Arc that associates with recycling endosomes assists in sorting γ-secretase from an intracellular source, (where it is enriched in tubulovesicular structures including presumptive sorting endosomes in dendrites) to early and recycling endosomes that process APP-CTF.

Notch is another well-characterized substrate of γ-secretase that is processed to generate transcription regulating peptide NICD. While Notch signaling is best characterized during development, Notch also plays a role in adult brain and is implicated in synaptic plasticity. A recent study demonstrates that Notch is processed to NICD in dendrites of mature neurons, and this is regulated by activity, and is dependent on Arc (Alberi et al., 2011). Notch processing is associated with endocytic trafficking, and the Arc/γ-secretase mechanism in the present study could underlie activity-dependent increases of γ-secretase processing of Notch.

Arc is best known for its role in trafficking of AMPA receptors and synaptic plasticity. Persistent activity that increases Arc expression in neuronal culture models or in visual cortex results in homeostatic downregulation of synaptic strength by increasing the rate of AMPA receptor endocytosis (Gao et al., 2010; Shepherd et al., 2006). The present study indicates that Arc induction also increases the generation of Aβ. Persistent aberrant activity as in the "default network" (Buckner et al., 2005) may underlie the increase of Arc that we detect in MFC in AD brains, and the effect of Arc to increase Aβ generation could contribute to the amyloid deposition associated with this activity (Sperling et al., 2009). Our studies validate the association between Arc-dependent Aβ generation and plaque deposition in an in vivo model. This link between Arc and AMPA receptor downregulation suggests that the persistence of aberrant activity in the default pathway in the AD brain may be indicative of failure of homeostatic scaling, which in a healthy brain would reestablish AMPA receptor dependent excitability and restore normal levels of activity. Arc could also be upregulated as part of a neuroinflammatory process (Rosi et al., 2005) or as a consequence of accumulation of Aβ oligomers (Lacor et al., 2004). We have confirmed that synthetic hAβ40 dimer can increase Arc expression in cultured neurons (Figures S7B–S7D), which suggests that Arc and Aβ oligomer could act in a positive feedback loop. The dual functions of Arc in the neural plasticity related to cognitive function, and Aβ generation, suggest a fundamental link between these processes that is disrupted in AD.

EXPERIMENTAL PROCEDURES

Mouse Strains

Both *Arc*$^{+/+}$ and *Arc*$^{-/-}$ mice are in congenic C57BL/6J background (Plath et al., 2006). Arc/Arg3.1 heterozygous mice (*Arc*$^{+/-}$) were crossed with AD mouse model (*APP*$_{SWE}$;*PS1ΔE9*) (C3H/HeJ * C57BL/6J, obtained from Dr. Philip Wong's lab) to generate *AD;Arc*$^{+/-}$ mice, which were backcrossed to *Arc*$^{+/-}$ to generate *AD;Arc*$^{+/+}$ and *AD; Arc* $^{-/-}$ mice. All procedures involving animals were under the guidelines of JHU Institutional Animal Care and Use Committee.

CoImmunoprecipitation, In Vitro Binding, Peptide Blocking Assay, and Surface Protein Trafficking Assay

Detailed protocols are provided in the Extended Experimental Procedures.

Immunoelectron Microscopy

Immuno-electron microscopy was performed by post-fixation immunogold labeling as described in detail in the Extended Experimental Procedures.

Aβ Assays on Mouse Brain

Brains of *AD;Arc*$^{+/+}$ and *AD;Arc*$^{-/-}$ mice were dissected on ice and homogenized in PBS buffer containing complete protease inhibitor cocktail (Roche). After the lysates were centrifuged at 100,000 x *g* for 30 min, the supernatants containing soluble Aβ peptides were collected for assay, and the pellets were homogenized in 70% formic acid solution. After incubation on ice for 1 hr, the formic acid lysates were centrifuged at 100,000 x *g* for 1 hr, and the supernatants were collected and neutralized by 1 M Tris-base solution. The concentrations of Aβ40/Aβ42 peptides in PBS-soluble and formic acid-soluble fractions were measured using a quantitative ELISA kit (Invitrogen) that specifically detects human Aβ40/Aβ42. BCA method was used to measure the total protein concentrations (Pierce).

Immunohistochemical Analysis of Amyloid Plaques in Mouse Brains

Mouse brains were fixed in 10% formaldehyde, dehydrated in methanol, treated with xylenes, and embedded in paraffin. The brain was cut parasagittally into 4 μm sections. Aβ load was measured in a parasagittal section immunostained with 6E10 antibody and counterstained with hematoxylin. Using the Stereo Investigator Optical Disector software (Version 7) from MBF Biosciences, we defined a contour that encompassed the whole cerebral cortex (excluding basal ganglia and hippocampus) with a grid size of 250 × 250 μm. The distance between the fractionator sampling sites was 10 μm. The fractional area occupied by Aβ immunoreactivity in the demarcated area was measured using the area fraction fractionator probe (AFF) with a 40x objective. Statistical differences between the fractional areas of Aβ in *AD;Arc*$^{+/+}$ and *AD;Arc*$^{-/-}$ mice were evaluated using the Mann-Whiteney U test.

Statistical Analysis

All data were analyzed statistically by Student's t test, two-tailed Mann-Whiteney U test and ANOVA with Turkey post hoc test using GraphPad Prism. All data are presented as mean ± SEM.

SUPPLEMENTAL INFORMATION

Supplemental Information includes Extended Experimental Procedures, one table, and seven figures and can be found with this article online at doi:10.1016/j.cell.2011.09.036.

ACKNOWLEDGMENTS

We would like to thank Gopal Thinakaran, Sangram Sisodia (University of Chicago), and Tong Li for critical reagents and helpful discussions. Thanks to Gay Rudow for helping with unbiased stereology. Thanks to Desheng Xu and Shi Yang for help with lentivirus packaging. Many thanks to Robert Ardiuni, Melissa Levesque, Darren Baker, and Stephan Miller from Biogen Idec for their excellent technical support on in vitro binding assay. We thank Ya-Xian Wang for help with the EM studies. We also thank Robert Malinow (University of California at San Diego) and Mike Ehlers (Duke University) for APP Sindbis virus constructs and GFP-Rab constructs. This work was supported by NIMH grant RO1 MH053608 (P.F.W.), the Johns Hopkins Alzheimer's Disease Research Center (NIH grant P50AG005146) and in part by the NIDCD Intramural Program (R. S. P.) and NIH grant MH084020.

Received: August 5, 2010
Revised: June 21, 2011
Accepted: September 21, 2011
Published: October 27, 2011

REFERENCES

Alberi, L., Liu, S., Wang, Y., Badie, R., Smith-Hicks, C., Wu, J., Pierfelice, T.J., Abazyan, B., Mattson, M.P., Kuhl, D., et al. (2011). Activity-induced Notch signaling in neurons requires Arc/Arg3.1 and is essential for synaptic plasticity in hippocampal networks. Neuron *69*, 437–444.

Buckner, R.L., Snyder, A.Z., Shannon, B.J., LaRossa, G., Sachs, R., Fotenos, A.F., Sheline, Y.I., Klunk, W.E., Mathis, C.A., Morris, J.C., and Mintun, M.A. (2005). Molecular, structural, and functional characterization of Alzheimer's disease: evidence for a relationship between default activity, amyloid, and memory. J. Neurosci. *25*, 7709–7717.

Capell, A., Grunberg, J., Pesold, B., Diehlmann, A., Citron, M., Nixon, R., Beyreuther, K., Selkoe, D.J., and Haass, C. (1998). The proteolytic fragments of the Alzheimer's disease-associated presenilin-1 form heterodimers and occur as a 100-150-kDa molecular mass complex. J. Biol. Chem. *273*, 3205–3211.

Chowdhury, S., Shepherd, J.D., Okuno, H., Lyford, G., Petralia, R.S., Plath, N., Kuhl, D., Huganir, R.L., and Worley, P.F. (2006). Arc/Arg3.1 interacts with the endocytic machinery to regulate AMPA receptor trafficking. Neuron *52*, 445–459.

Cirrito, J.R., Kang, J.E., Lee, J., Stewart, F.R., Verges, D.K., Silverio, L.M., Bu, G., Mennerick, S., and Holtzman, D.M. (2008). Endocytosis is required for synaptic activity-dependent release of amyloid-beta in vivo. Neuron *58*, 42–51.

Cirrito, J.R., Yamada, K.A., Finn, M.B., Sloviter, R.S., Bales, K.R., May, P.C., Schoepp, D.D., Paul, S.M., Mennerick, S., and Holtzman, D.M. (2005). Synaptic activity regulates interstitial fluid amyloid-beta levels in vivo. Neuron *48*, 913–922.

Costes, S.V., Daelemans, D., Cho, E.H., Dobbin, Z., Pavlakis, G., and Lockett, S. (2004). Automatic and quantitative measurement of protein-protein colocalization in live cells. Biophys. J. *86*, 3993–4003.

Cracchiolo, J.R., Mori, T., Nazian, S.J., Tan, J., Potter, H., and Arendash, G.W. (2007). Enhanced cognitive activity–over and above social or physical activity–is required to protect Alzheimer's mice against cognitive impairment, reduce Abeta deposition, and increase synaptic immunoreactivity. Neurobiol. Learn. Mem. *88*, 277–294.

De Strooper, B., and Annaert, W. (2010). Novel research horizons for presenilins and gamma-secretases in cell biology and disease. Annu Rev Cell Dev Biol. *26*, 235–260.

Gao, M., Sossa, K., Song, L., Errington, L., Cummings, L., Hwang, H., Kuhl, D., Worley, P., and Lee, H.K. (2010). A specific requirement of Arc/Arg3.1 for visual experience-induced homeostatic synaptic plasticity in mouse primary visual cortex. J. Neurosci. *30*, 7168–7178.

Hardy, J., and Selkoe, D.J. (2002). The amyloid hypothesis of Alzheimer's disease: progress and problems on the road to therapeutics. Science *297*, 353–356.

Huse, J.T., Pijak, D.S., Leslie, G.J., Lee, V.M., and Doms, R.W. (2000). Maturation and endosomal targeting of beta-site amyloid precursor protein-cleaving enzyme. The Alzheimer's disease beta-secretase. J. Biol. Chem. *275*, 33729–33737.

Jankowsky, J.L., Slunt, H.H., Ratovitski, T., Jenkins, N.A., Copeland, N.G., and Borchelt, D.R. (2001). Co-expression of multiple transgenes in mouse CNS: a comparison of strategies. Biomol. Eng. *17*, 157–165.

Kamenetz, F., Tomita, T., Hsieh, H., Seabrook, G., Borchelt, D., Iwatsubo, T., Sisodia, S., and Malinow, R. (2003). APP processing and synaptic function. Neuron *37*, 925–937.

Lacor, P.N., Buniel, M.C., Chang, L., Fernandez, S.J., Gong, Y., Viola, K.L., Lambert, M.P., Velasco, P.T., Bigio, E.H., Finch, C.E., et al. (2004). Synaptic targeting by Alzheimer's-related amyloid beta oligomers. J. Neurosci. *24*, 10191–10200.

Lazarov, O., Robinson, J., Tang, Y.P., Hairston, I.S., Korade-Mirnics, Z., Lee, V.M., Hersh, L.B., Sapolsky, R.M., Mirnics, K., and Sisodia, S.S. (2005). Environmental enrichment reduces Abeta levels and amyloid deposition in transgenic mice. Cell *120*, 701–713.

Levitan, D., Lee, J., Song, L., Manning, R., Wong, G., Parker, E., and Zhang, L. (2001). PS1 N- and C-terminal fragments form a complex that functions in APP processing and Notch signaling. Proc. Natl. Acad. Sci. USA *98*, 12186–12190.

Lewis, S.J., Smith, A.L., Neduvelil, J.G., Stevenson, G.I., Lindon, M.J., Jones, A.B., Shearman, M.S., Beher, D., Clarke, E., Best, J.D., et al. (2005). A novel series of potent gamma-secretase inhibitors based on a benzobicyclo[4.2.1] nonane core. Bioorg. Med. Chem. Lett. *15*, 373–378.

Park, S., Park, J.M., Kim, S., Kim, J.A., Shepherd, J.D., Smith-Hicks, C.L., Chowdhury, S., Kaufmann, W., Kuhl, D., Ryazanov, A.G., et al. (2008). Elongation factor 2 and fragile X mental retardation protein control the dynamic translation of Arc/Arg3.1 essential for mGluR-LTD. Neuron *59*, 70–83.

Plath, N., Ohana, O., Dammermann, B., Errington, M.L., Schmitz, D., Gross, C., Mao, X., Engelsberg, A., Mahlke, C., Welzl, H., et al. (2006). Arc/Arg3.1 is essential for the consolidation of synaptic plasticity and memories. Neuron *52*, 437–444.

Ribaut-Barassin, C., Moussaoui, S., Brugg, B., Haeberle, A.M., Huber, G., Imperato, A., Delhaye-Bouchaud, N., Mariani, J., and Bailly, Y.J. (2000). Hemisynaptic distribution patterns of presenilins and beta-APP isoforms in the rodent cerebellum and hippocampus. Synapse *35*, 96–110.

Rosi, S., Ramirez-Amaya, V., Vazdarjanova, A., Worley, P.F., Barnes, C.A., and Wenk, G.L. (2005). Neuroinflammation alters the hippocampal pattern of behaviorally induced Arc expression. J. Neurosci. *25*, 723–731.

Shelton, C.C., Tian, Y., Frattini, M.G., and Li, Y.M. (2009). An exo-cell assay for examining real-time gamma-secretase activity and inhibition. Mol. Neurodegener. *4*, 22.

Shepherd, J.D., Rumbaugh, G., Wu, J., Chowdhury, S., Plath, N., Kuhl, D., Huganir, R.L., and Worley, P.F. (2006). Arc/Arg3.1 mediates homeostatic synaptic scaling of AMPA receptors. Neuron *52*, 475–484.

Small, S.A., and Gandy, S. (2006). Sorting through the cell biology of Alzheimer's disease: intracellular pathways to pathogenesis. Neuron *52*, 15–31.

Sperling, R.A., Laviolette, P.S., O'Keefe, K., O'Brien, J., Rentz, D.M., Pihlajamaki, M., Marshall, G., Hyman, B.T., Selkoe, D.J., Hedden, T., et al. (2009). Amyloid deposition is associated with impaired default network function in older persons without dementia. Neuron *63*, 178–188.

Thinakaran, G., and Koo, E.H. (2008). Amyloid precursor protein trafficking, processing, and function. J. Biol. Chem. *283*, 29615–29619.

Tian, Y., Bassit, B., Chau, D., and Li, Y.M. (2010). An APP inhibitory domain containing the Flemish mutation residue modulates gamma-secretase activity for Abeta production. Nat. Struct. Mol. Biol. *17*, 151–158.

Vetrivel, K.S., Cheng, H., Kim, S.H., Chen, Y., Barnes, N.Y., Parent, A.T., Sisodia, S.S., and Thinakaran, G. (2005). Spatial segregation of gamma-secretase and substrates in distinct membrane domains. J. Biol. Chem. *280*, 25892–25900.

Vetrivel, K.S., and Thinakaran, G. (2006). Amyloidogenic processing of beta-amyloid precursor protein in intracellular compartments. Neurology *66*, S69–73.